Preparation and Mechanical and Electrical Properties of Graphene Nanosheets–Poly(methyl methacrylate) Nanocomposites via *In Situ* Suspension Polymerization

Jingchao Wang,[1] Huating Hu,[1] Xianbao Wang,[1,2] Chunhui Xu,[1] Min Zhang,[1] Xiaopeng Shang[1]

[1]*Ministry-of-Education Key Laboratory for the Green Preparation and Application of Functional Materials, Hubei University, Wuhan 430062, People's Republic of China*
[2]*Faculty of Materials Science and Engineering, Hubei University, Wuhan 430062, People's Republic of China*

Received 19 July 2010; accepted 31 January 2011
DOI 10.1002/app.34284
Published online 10 June 2011 in Wiley Online Library (wileyonlinelibrary.com).

ABSTRACT: Graphene nanosheets–poly(methyl methacrylate) (GNS–PMMA) nanocomposites were first prepared by *in situ* suspension polymerization and reduction of graphene oxide using hydrazine hydrate and ammonia. PMMA microspheres with a mean diameter of 2 μm are mainly covalently link to the surface of GNS. The obtained GNS–PMMA composites have not only high electrical conductivity but also enhanced mechanical properties and thermal stability at low loadings of graphene. Especially, the resulting nanocomposites were examined for electrorheological fluids, showing thin and dense chains of particles after application of an electric field. © 2011 Wiley Periodicals, Inc. J Appl Polym Sci 122: 1866–1871, 2011

Key words: graphene; PMMA; nanocomposites; electrical properties; electrorheological property

INTRODUCTION

Graphene, a one-atom-thick planar sheet of sp^2-bonded carbon atoms that are densely packed in a honeycomb crystal lattice, has attracted significant interests owing to its extraordinary properties and potential applications in various areas, since its first discovery in 2004.[1–3] No previous material has displayed the combination of superlative mechanical, thermal, and electronic properties attributed to them.[4–6] These properties make graphene ideal not only for a wide range of applications but also as a test bed for fundamental science.

Recent interest in graphene–polymer nanocomposites has grown significantly because of the unique properties of graphene. Stankovich et al.[7] reported that the graphene/polystyrene (PS) nanocomposite showed the lowest percolation threshold of 0.1% (v/v) for room temperature electrical conductivity amongst the different carbon nanostructures, and the composites showed 10^{-3} S cm^{-1} conductivity at only 1% (v/v) of graphene, which is sufficient for many electrical applications. Poly(methyl methacrylate) (PMMA) is a common polymer often used on a macroscale as a sheet glass substitute due to its low cost, good processing temperature range, and ability to be molded into mostly any shape. There are some literatures that reported carbon nanotubes (CNTs)/PMMA nanocomposite. Goncalves et al.[8] successfully modified the surface of graphene oxide (GO) with PMMA chains via atom transfer radical polymerization. The resulting nanocomposites were readily dispersed in organic solvents such as chloroform. Pramoda et al.[9] explored a route to the synthesis of covalently bonded PMMA/graphene nanocomposites *in situ* bulk polymerization and the consequent enhancement in thermal stability properties, when the content of graphene is 0.5 wt %.

Our laboratory prepared and examined graphene nanocomposites with various polymers such as PS, polyvinyl alcohol, and low-density polyethylene, which were synthesized by situ emulsion polymerization, solution mixing, and melt mixing, respectively.[10–12] During these studies, we found that the fine dispersion of graphene in a polymer matrix enhanced not only the thermal stability and mechanical properties but also the barrier properties was obviously improved. In this article, we reported a new, simple, and efficient route for preparing graphene nanosheets (GNS)–PMMA nanocomposites via *in situ* suspension polymerization. The obtained GNS–PMMA composites exhibited significant enhancement of mechanical properties and thermal stability at a low loadings of graphene. Furthermore,

Correspondence to: X. B. Wang (wangxb68@yahoo.com.cn).
Contract grant sponsor: National Natural Science Foundation of China; contract grant number: 50772031.
Contract grant sponsor: Hubei Provincial Department of Science & Technology; contract grant number: 2009CDA021.

we have investigated the electrorheological (ER) characteristic of the as-prepared nanocomposites when dispersed in silicone oil under an applied electric field.

EXPERIMENTAL

Materials

Natural flake graphite was supplied by Shandong Qingdao Company (China). Methyl methacrylate (MMA), 2,2-azobisisobutyronitrile (AIBN), poly(*N*-vinylpyrrolidone) (PVP), methanol, ethanol, acetone, tetrahydrofuran (THF), ammonia, and hydrazine hydrate ($N_2H_4 \cdot H_2O$) were obtained from Shanghai Chemical Company (China). MMA was purified before use. Other reagents were obtained from commercial sources and were used as received.

Synthesis of GO and GNS

Natural graphite powders were oxidized to GO using our earlier methed.[10] In a typical synthesis process, 3 g graphite powder and 3 g sodium nitrate were put into 150 mL concentrate H_2SO_4 (in an ice bath). Afterward, 9 g $KMnO_4$ was gradually added. The mixture was then transferred to a 40°C water bath and stirred for about 2 h, forming a thick paste. Subsequently, 150 mL deionized water was added gradually. After 20 min, 30 mL 80% H_2O_2 solution was added to the mixture to reduce the residual $KMnO_4$. The mixture was stirred for another 10 min, and then diluted with 700 mL deionized water. The solution was then filtered and washed with deionized water until the pH was 7 and dried at room temperature under vacuum to obtain GO solid.

GNS were obtained by reduction of GO nanosheets using hydrazine hydrate and ammonia as reducing agent at 100°C for 4 h. In a typical synthesis procedure, about 350 mg GO was dispersed in 350 mL deionized water and then exfoliated to generate GO by ultrasonication for 1 h. Subsequently, 5 mL 80% hydrazine hydrate and 5 mL ammonia were added to the solution. After heated at 100°C for 4 h, the mixture turned from a yellowish brown solution to a black suspension. The mixture was then cooled and filtered and washed several times with deionized water. The product was dried at 50°C under vacuum overnight to obtain GNS.

Preparation of GNS–PMMA nanocomposites

A typical synthesis procedure for the GNS–PMMA nanocomposites with GO loadings from 0 to 2 wt % were as follows: A certain amount of GO powers were dispersed in deionized water and ultrasonicated for 20 min. To examine the effect of GO contents on the composite properties, we formulated the GO contents of 0, 0.5, 1, 1.5, and 2 wt % with respect to the PMMA content. Then 1 g PVP and 20 g MMA monomer were added into the GO colloid dispersion, followed by 15 min of ultrasonic irradiation. Afterward, 0.2 g AIBN radical initiator dispersed in 250 mL methanol was added into the mixture and the reaction mixture was refluxed at 80°C for 10 h under a nitrogen atmosphere. Then, 2 mL of hydrazine and 2 mL of ammonia were added to the suspension and the reaction mixture was again refluxed at 100°C for 4 h, leading to the formation of the GNS–PMMA nanocomposites. The resulted black suspension was cooled to room temperature and then filtered through a 0.22-μm polytetrafluoroethylene (PTFE) membrane and washed with abundant demonized water and ethanol several times to remove impurities. The purified product was dried in vacuum oven at 60°C to get dried GNS–PMMA nanocomposites as a grayish black solid. The pristine PMMA microspheres were synthesized in the absence of graphene oxide nanosheets (GONS) using the same method under the same experimental conditions.

Characterization and measurements

Fourier transform infrared spectra (FTIR, TJ270-30) were recorded by using KBr as a background on a Perkin-Elmer Spectrum One spectrometer. Raman spectra were measured on a Lab RAM HR 800 UV (HORIBA Jobin Yvon, France) multichannel confocal microspectrometer with 633 nm laser excitation. Scanning was taken on an extended range (800–3000 cm^{-1}) and the exposure time was 50 s. The solid samples were scanned directly, and three tests were conducted for each sample. Thermogravimetric analyses (TGA) of the samples was done under nitrogen environment using a Perkin-Elmer TGA-7 instrument at a heating rate of 10°C min^{-1}. Solubility measurements were carried out through dispersing the samples into acetone and THF by an ultrasonic generator. Dynamic mechanical thermal analysis for the samples was performed from 10 to 200°C with a solid-state analyzer RSA II (Rheometrics Scientific system). Temperature scans at a frequency of 1 Hz were carried out with a heating rate of 3°C min^{-1}. The morphologies and structures of the samples were examined with field emission scanning electron microscope (SEM) operated on a Nova 400 Nano SEM. The mechanical properties of GNS–PMMA nanocomposites were measured using a universal testing machine (CMT-4104, SANS Group, China) at room temperature. A load cell of 500 N was used and the tensile rate imposed was 30 mm min^{-1}. All the samples were molded to a rectangular shape ($50 \times 10 \times 2$ mm^2). More than three tests were

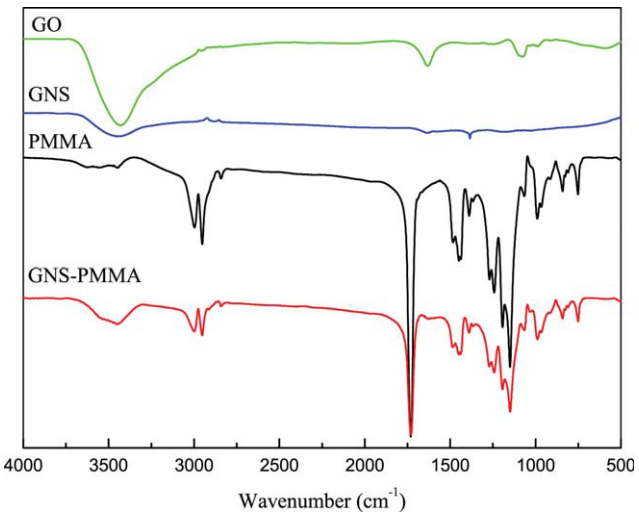

Figure 1 FTIR spectra of GO, GNS, PMMA, and GNS–PMMA nanocomposites. [Color figure can be viewed in the online issue, which is available at wileyonlinelibrary.com.]

conducted for each sample from which the mean values and standard deviations were derived. Electrical conductivity of the nanocomposites was measured by a four-probe method using pressed disc-type specimens at room temperature. The ER fluids were prepared by sonication using the dried GNS–PMMA nanocomposites dispersed in silicone oil (1.2 wt %). No stabilizers were added to the silicone oil. A DC high voltage source was used to apply to the samples. The gap between the two parallel electrodes was fixed at 5 mm. The images of the ER fluids were obtained using a digital camera.

RESULTS AND DISCUSSIONS

It has been reported by our and Choi's groups that during the *in situ* suspension polymerization, the radical AIBN can not only initiate the polymerized reaction of MMA but also open the π-bonds of CNT,[13,14] resulting in the grafting of polymer chains onto the CNT surface caused via either direct polymerization of MMA at the opened π-bond or by attachment of oligomeric PMMA chains. When compared with CNT, graphene possesses similar physical properties but larger surface areas, which can be considered as an unrolled CNT.[15] The results from FTIR spectra were performed to determine the interaction between PMMA matrix and graphene sheets. As shown in Figure 1, the exfoliated GO exhibits three characteristic peaks at 3443, 1660, and 1089 cm^{-1}, indicating the presence of the hydroxyl, benzene carboxyl, and epoxy groups, respectively. The FTIR spectrum of graphene only exhibits one characteristic peak at 3443 cm^{-1}. The existence of hydroxyl groups may be due to the incomplete reduction of GO. After *in situ* suspension polymerization, the FTIR spectrum of GNS–PMMA not only has the characteristic peaks of PMMA (3007 and 2920 cm^{-1} for C—H stretching, 1730 cm^{-1} for C=O stretching, and 1190 and 1150 cm^{-1} for C—O stretching) but also has the peaks of exfoliated GO (3450 cm^{-1} for O—H stretching, which may be due to the incomplete reduction of GO). All in all, these FTIR results provide direct evidence for covalent bonding among GNS and PMMA.

Raman spectrum also provides essential information for evaluating the covalent modification of the GNS. The Raman spectra for the purified GNS shown in Figure 2 displays characteristic D band at 1355 cm^{-1} and G band at 1594 cm^{-1}.The D band is related to the sp^3 states of carbon, and it is used as a proof of disruption of the aromatic π-electrons system of GNS. The intensity ratios of the D–G band (I_D/I_G) for the GNS–PMMA composites is 1.50, which are larger than those of the purified GNS (1.03), indicating sp^2 hybridized carbons have been converted to sp^3 hybridization carbons because of the covalent attachment of the PMMA chains onto the surface of GNS.

The successful covalent functionalization of GNS is also reflected by TGA. As seen in Figure 3, it can be observed that GO is not thermally stable and starts to lose mass on heating even below 100°C; the major mass loss occurs at 160°C, which may be attributed mass loss to the pyrolysis of the labile oxygen-containing functional groups such as —OH, —COOH, etc. After chemical reduction, the thermally labile oxygen functional groups were removed, and the thermal stability of GNS was improved. In addition, the main-chain pyrolysis of PMMA in the GNS–PMMA nanocomposites shifts to a higher temperature than that of pure PMMA, indicating that

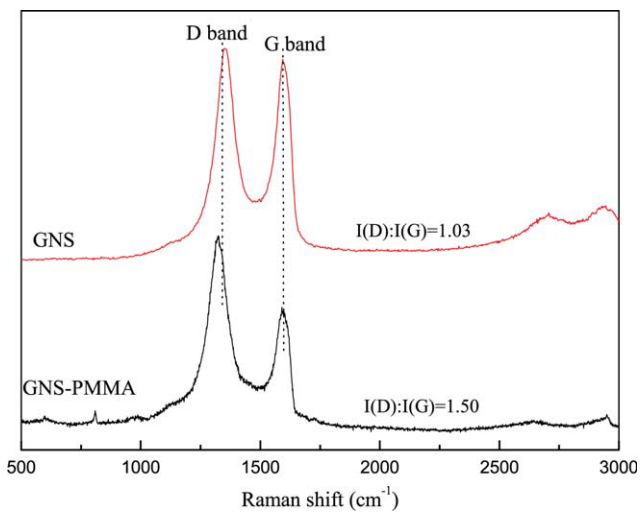

Figure 2 Raman spectra of GNS and GNS–PMMA nanocomposites. [Color figure can be viewed in the online issue, which is available at wileyonlinelibrary.com.]

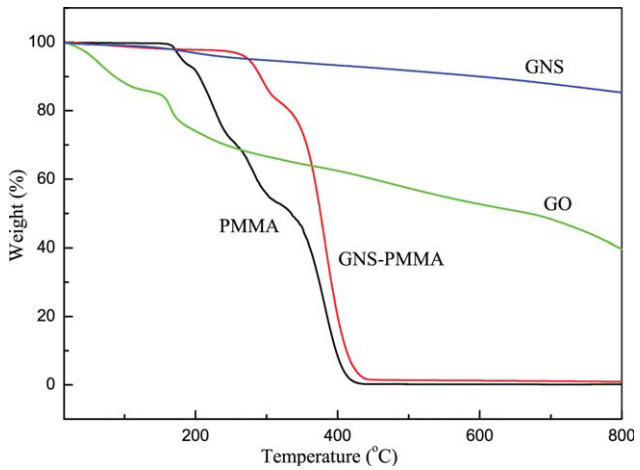

Figure 3 TGA curves of GO, GNS, PMMA, and GNS–PMMA nanocomposites. [Color figure can be viewed in the online issue, which is available at wileyonlinelibrary.com.]

the presence of GNS has remarkably enhanced the thermal stability of PMMA. Furthermore, the content of GNS is about 1 wt % in the composites. In addition, the four-probe electrical measurements gave a DC conductivity of 1.6×10^{-5} S cm^{-1} for GNS–PMMA nanocomposites, much higher than that of pure PMMA (1.3×10^{-13} S cm^{-1}) reported by an earlier research.[16]

The loss tangent and storage modulus of neat PMMA and 1 wt % GNR–PMMA as a function of temperature were shown in Figure 4. As we all known, the glass transition temperature (T_g) is defined as the temperature at which a maximum of tanδ is observed, which is a common practice for polymer materials. It could be observed that the T_g of neat PMMA increased from 123 to 132°C for the GNR–PMMA nanocomposites with 1 wt % loadings. The contribution to the increase of T_g could be two factors: (1) restriction in chain mobility because of confinement effect of 2D-layered graphenes and (2) chemical bond of one end of PMMA molecular chains to graphene surfaces.[9]

To investigate the morphology of GNS, PMMA, and GNS–PMMA, SEM measurements have also been performed. As shown in Figure 5, the as-prepared GNS [Fig. 5(a)] look like thin "petal" with a typical lamella structure and they are crumpled and wrinkled due to the van der Waals interactions. The PMMA microspheres have a perfect spherical structure with an average diameter of 2 μm [Fig. 5(b)]. As for GNS–PMMA composites [Figs. 4(d) and 5(c)], we can distinctly find that many PMMA microspheres are firmly immobilized on or anchored to the GNS, which further confirm the successful decoration of GNS by PMMA microspheres.

The homogeneity of composites and the stronger interfacial interaction between nanomaterials and polymer matrix have a significant effect on the mechanical properties. Typical stress–strain behaviors for the GNR–PMMA composites varying graphene loadings were presented in Figure 6. It was obvious that the addition of graphene into the polymer matrix had a significant influence on the mechanical behavior. As shown in Figure 6, the tensile strength increased with increasing GO loadings. When the loading of graphene was 1 wt%, the tensile strength and elongation at break reached the maximum and increased by 60.7% and 62.8%, respectively, when compared with pure PMMA. However, increasing the concentration of GNR to about 2 wt % deteriorated the mechanical behavior of the overall composite. This may be due to the agglomeration of graphene sheets creating defects in the PMMA matrix composite. Similar downturns of the mechanical properties of composites have been reported and attributed to aggregation and percolation effects.[8]

The solubility of the samples was shown in Figure 7(A). GNS dispersed in acetone (a) and THF (b) began to precipitate immediately after sonication. However, the PMMA-decorated GNS remain stable after prolonged standing (3 h) in acetone (c) and THF (d). This behavior arises from the formation of a network, where the soluble PMMA chains extend into the solution and create high steric hindrance and prevent the GNS from approaching each other. For comparison, the direct mixture of PMMA microspheres and GNS became unstable within 5 min followed by the precipitation of GNS and the dissolution of PMMA in the solvents, as shown in Figure 5(A(e)) and Figure 7(A(f)), further demonstrating that PMMA link to the surface of GNS mainly through a covalent bond rather than noncovalent interaction such as electrostatic interaction.

The ER behaviors of GNS–PMMA nanocomposites are shown in Figure 7(B). Without an applied electric

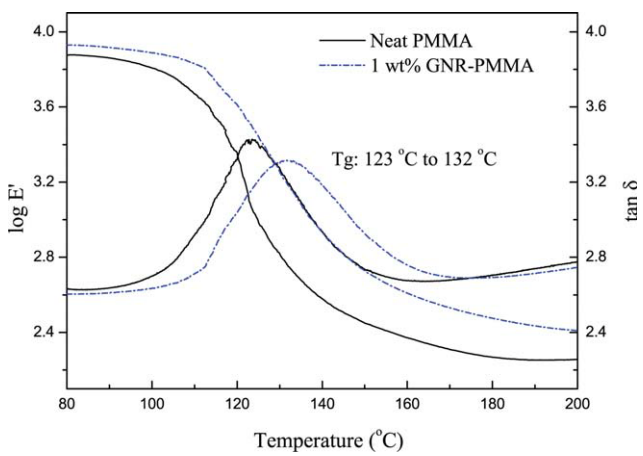

Figure 4 Dynamic mechanical analyses of neat PMMA and 1 wt % GNR–PMMA. [Color figure can be viewed in the online issue, which is available at wileyonlinelibrary.com.]

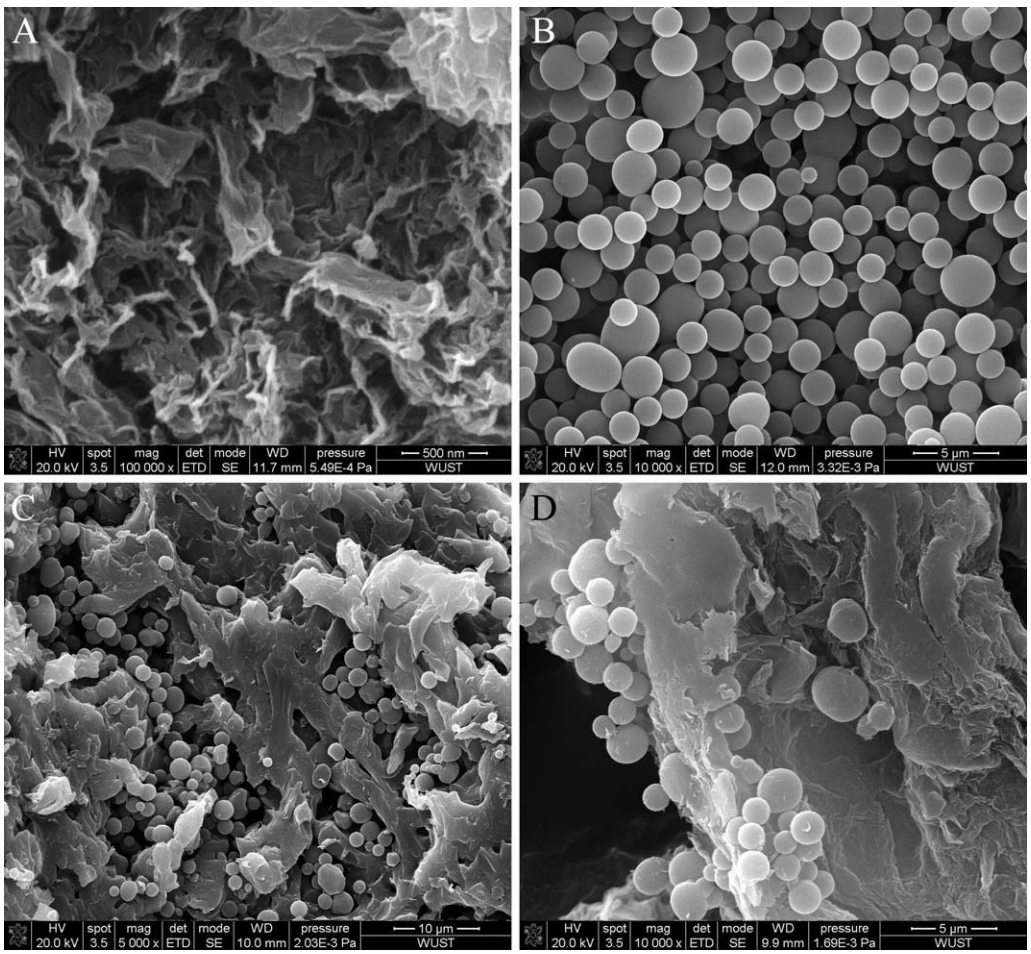

Figure 5 SEM images: (A) GNS, (B) PMMA, and (C, D) GNS–PMMA nanocomposites.

field, the nanocomposites were randomly dispersed in silicone oil as a Newtonian fluid.[16] However, when an electric field (1.2 kV cm^{-1}) was applied, it formed typical structures of ER materials with thin and dense chains of particles along the orientation of the applied electric fields. The structure remained stable as long as the electric fields were applied. It is possible that the fibrillated chains structure might provide a path for the mobile carrier transporting, which determines the conducting behavior of ER fluids.[16–18]

CONCLUSIONS

The GNS–PMMA nanocomposites were successfully prepared via *in situ* dispersion polymerization and reduction of GO using hydrazine hydrate and ammonia. This procedure is a promising route for the production of composite materials based on graphene, in which graphene sheets are expected to play an important role in the near future. PMMA microspheres are mainly covalently linked to the surface of GNS, which disrupted the van der Waals interactions and leaded to a perfect dispersion of GNS in conventional polar organic solution. The synthesized composites exhibited a significant improvement in thermal stability, electrical

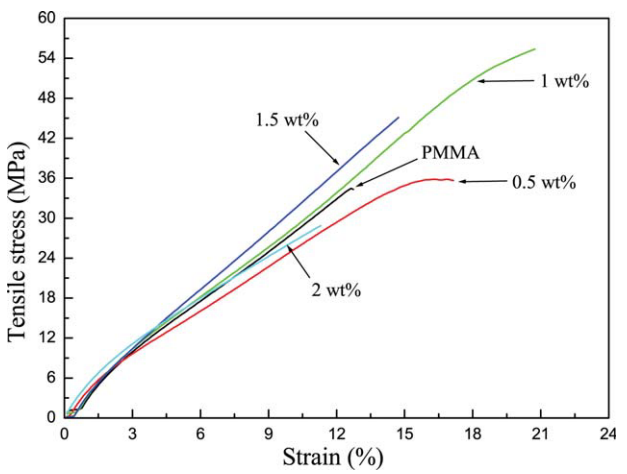

Figure 6 Typical stress–strain curves of the GNR–PMMA composites with varying GNR loadings. [Color figure can be viewed in the online issue, which is available at wileyonlinelibrary.com.]

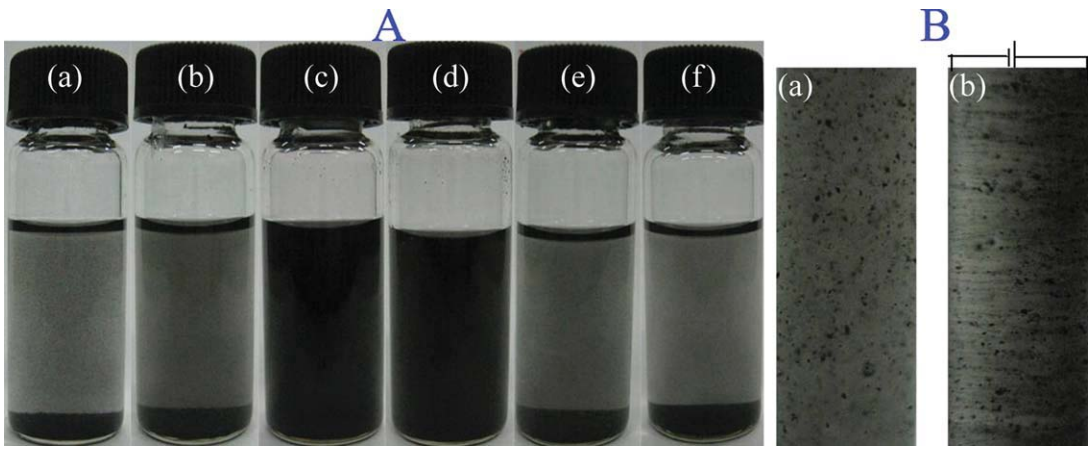

Figure 7 (A) Photographs of different samples with the same GNS concentration of 1 mg mL^{-1}: GNS in acetone (a) and THF (b), GNS–PMMA in acetone (c) and THF (d), mixtures of GNS and PMMA in acetone (e) and THF (f); (B) ER behaviors of GNS–PMMA nanocomposites dispersed in silicon oil (1.2 wt %) between two electrodes under an applied electric field of (a) 0 kV cm^{-1} and (b) 1.2 kV cm^{-1}. [Color figure can be viewed in the online issue, which is available at wileyonlinelibrary.com.]

properties, and mechanical properties at a low loading of graphene. Reinforcement with graphene resulted in increase of up to 60.7% and 62.8% in the tensile strength and elongation at break of the nanocomposites, respectively, when compared with pure PMMA. Moreover, the as-prepared nanocomposites showed ER fluid characteristics when dispersed in silicone oil under an applied electric field. It is believed that the PMMA-decorated GNS nanocomposites will hold prospective applications in many different areas.

References

1. Novoselov, K. S.; Geim, A. K.; Morozov, S. V. Science 2004, 306, 666.
2. Geim, A. K.; Novoselov, K. S. Nat Mater 2007, 6, 183.
3. Eda, G.; Fanchini, G.; Chhowalla, M. Nat Nanotechnol 2008, 3, 270.
4. Park, S.; Ruoff, R. S. Nat Nanotechnol 2009, 4, 217.
5. Li, D.; Müller, M. B.; Gilje, S.; Kaner, R. B.; Wallace, G. G. Nat Nanotechnol 2008, 3, 101.
6. Geim, A.K. Science 2009, 324, 1530.
7. Stankovich, S.; Dikin, A. D.; Dommett, G. H. B.; Kohlhaas, K. M.; Zimney, E. J.; Stach, E. A.; Piner, R. D.; Nguyen, S. T.; Ruoff, R. S. Nature 2006, 442, 282.
8. Goncalves, G.; Marques, P.; Timmons, A. B.; Bdkin, I.; Singh, M. K.; Emami, N.; Grácio, J. J Mater Chem 2010, 20, 9927.
9. Pramoda, K. P.; Hussain, H.; Koh, H. M.; Tan, H. R.; He, C. B. J Polym Sci Polym Chem 2010, 48, 4262.
10. Hu, H. T.; Wang, X. B.; Wang, J. C.; Wan, L.; Liu, F. M.; Zheng, H.; Chen, R.; Xu, C. H. Chem Phys Lett 2010, 484, 247.
11. Wang, J. C.; Xu, C. H.; Hu, H. T.; Wan, L.; Chen, R.; Zheng, H.; Liu, F. M.; Zhang, M.; Shang, X. P.; Wang, X. B. J Nano Res 2011, 13, 869.
12. Wang, J. C.; Wang, X. B.; Xu, C.H.; Zhang, M.; Shang, X. P. Polym Int 2011, DOI 10.1002/pi.3025.
13. Li, M. J.; Wang, X. B.; Tian, R.; Liu, F. M.; Hu, H. T.; Chen, R.; Zheng, H.; Wan, L. Compos Part A Appl Sci Manuf 2009, 40, 413.
14. Park, S. J.; Cho, M. S.; Lim, S. T.; Choi, H. J. Macromol Rapid Commun 2005, 26, 1563.
15. Dikin, D. A.; Stankovich, S. Nature 2007, 448, 457.
16. Lee, I. S.; Yoon, S. H.; Jin, H. J.; Choi, H. J. Diam Relat Mater 2006, 15, 1094.
17. Kwon, S.; Kim, H.; Myung, S. J.; Jin, H. J. J Polym Sci Part B: Polym Phys 2008, 46, 182.
18. Jin, H. J.; Choi, H. J.; Yoon, S. H.; Myung, S. J. Chem Mater 2005, 17, 4034.